Hindawi Publishing Corporation
Journal of Nanomaterials
Volume 2014, Article ID 534105, 7 pages
http://dx.doi.org/10.1155/2014/534105

Research Article

Bilayer Graphene Application on NO_2 Sensor Modelling

Elnaz Akbari,[1] R. Yusof,[1] M. T. Ahmadi,[2,3] A. Enzevaee,[4] M. J. Kiani,[2] H. Karimi,[5] and M. Rahmani[2]

[1] *Centre for Artificial Intelligence and Robotics (CAIRO), Universiti Teknologi Malaysia, 54100 Jalan Semarak, Kuala Lumpur, Malaysia*
[2] *Computational Nanoelectronic Research Group Faculty of Electrical Engineering, Universiti Teknologi Malaysia, 81310 Johor, Malaysia*
[3] *Nanotechnology Research Center Nanoelectronic Group, Physics Department, Urmia University, Urmia 57147, Iran*
[4] *Faculty of Mechanical Engineering, Universiti Teknologi Malaysia, 81310 Johor, Malaysia*
[5] *Malaysia-Japan International Institute of Technology (MJIIT), Universiti Teknologi Malaysia, 54100 Jalan Semarak, Kuala Lumpur, Malaysia*

Correspondence should be addressed to R. Yusof; rubiyah@ic.utm.my

Received 11 September 2013; Accepted 9 January 2014; Published 24 April 2014

Academic Editor: Razali Ismail

Graphene is one of the carbon allotropes which is a single atom thin layer with sp^2 hybridized and two-dimensional (2D) honeycomb structure of carbon. As an outstanding material exhibiting unique mechanical, electrical, and chemical characteristics including high strength, high conductivity, and high surface area, graphene has earned a remarkable position in today's experimental and theoretical studies as well as industrial applications. One such application incorporates the idea of using graphene to achieve accuracy and higher speed in detection devices utilized in cases where gas sensing is required. Although there are plenty of experimental studies in this field, the lack of analytical models is felt deeply. To start with modelling, the field effect transistor- (FET-) based structure has been chosen to serve as the platform and bilayer graphene density of state variation effect by NO_2 injection has been discussed. The chemical reaction between graphene and gas creates new carriers in graphene which cause density changes and eventually cause changes in the carrier velocity. In the presence of NO_2 gas, electrons are donated to the FET channel which is employed as a sensing mechanism. In order to evaluate the accuracy of the proposed models, the results obtained are compared with the existing experimental data and acceptable agreement is reported.

1. Introduction

Currently, there are various kinds of hazardous gases which are harmful to the organic life and are difficult to observe and sense [1–3]. Therefore, a sensor or a detection system is a necessary component in environments where human presence is inevitable. In the case of gas sensors, the best sensor would be defined as one that is able to detect even one molecule or atom of the chemical or gas [4–6]. Gas sensor efficiency can be improved significantly by the state-of-the-art technology [7–11]. Sensor technology has become omnipresent in the modern life, and nanosensor provides the foundation for highly developed electronic technology. According to the studies, graphene is one of the crystalline allotropes by two-dimensional network of carbon atoms arranged on a honeycomb structure [12–14]. Also, graphene has been widely implemented for the detection of various chemical materials including NO_2, NH_3, CO_2, H_2O, and CO because of its excellent adsorption properties and carrier mobility [15, 16]. Bilayer graphene (BLG) is the stack of two graphene layers, due to special features such as electrical, physical, and optical properties, and is known as an appropriate material to be used in nanotechnology especially in the sensor area [17, 18].

The twisted configuration and Bernal stacking are two common structures of bilayer graphene. In the former, the layers are rotating toward each other while, in the latter, half of the carbon atoms in one layer are standing over the other half [19, 20]. The electrical and optical features of bilayer graphene can be influenced by orientation and stacking order. The AA-stacked configuration is metallic, but the AB-stacked configuration, which is in our focus, behaves

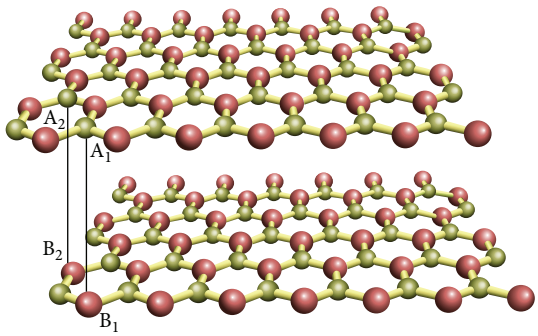

Figure 1: The schematic of bilayer graphene (AB-stacked configuration).

like a semiconductor material [21, 22]. In the AB structure of bilayer graphene with hexagonal carbon lattice, the atoms located on the top layer of BLG are A_1 and A_2, whereas atoms on the bottom layer of BLG are labelled B_1 and B_2 [18] as shown in Figure 1.

One of the most interesting properties in BLG is its band structure. Through theoretical studies it has been assumed that, by applying a perpendicular electric field, the band gap can be induced by reducing the asymmetry of two graphene layers in the BLG [19]. The controllable band gap is one of the most excellent properties of BLG that makes it a promising material in nanotechnology. In Figure 2(a), the band structure of the unbiased BLG with no external perpendicular electric fields is shown. It demonstrates that the BLG is a zero gap semiconductor with four parabolic bands, where two inner bands contact each other near the Dirac points at zero energy and the two outer bands are separated by the interlayer hopping energy, $\pm\, t$ [23, 24].

In the biased BLG, as shown in Figure 2(b), by applying a perpendicular electric field, a band gap is opened which is given by [26]

$$E_g = \frac{Vt_\perp}{\sqrt{V^2 + t_\perp^2}}, \tag{1}$$

where $V = V_1 - V_2$ is the potential energy difference between the first and second layers and V_1 and V_2 are the potential energy of the first and second layers, respectively. The parameter V can be controlled externally; therefore, by adjusting V, the band gap can be tuned [25].

2. The Proposed Model

The sensitivity of graphene to the miniature applied voltage can be used in sensor technology. In Figure 3, nanosensor detection method is illustrated schematically. In this model, the bilayer graphene as a substrate of gas sensor has been used. As can be seen in the figure, it looks similar to the conventional field effect transistors (FET) which include a source metal, a drain metal, a silicon back gate, and a gate insulator [27]. A graphene channel connects the source and drain electrodes, a dielectric barrier layer (SiO_2) separates the gate from the channel, and SiO_2 is used under the graphene as a dielectric layer while silicon acts as a back gate. When gas molecules attach to the surface or edges of CNT, carrier concentration will change. Due to this variability, the drain source current is a measurable parameter. This platform is employed in our model as a FET-based sensor structure [28].

The threshold voltage (V_{TH}) of a MOSFET is usually defined as the gate voltage where an inversion layer forms at the interface between the insulating layer (oxide) and the substrate (body) of the transistor. MOSFET is a device used for amplifying or switching electronic signals. When the gate-source voltage is smaller than the threshold voltage ($V_{GS} < V_{TH}$), there will be no conduction between the source and the drain, and the switch will be off. In contrast, when $V_{GS} > V_{TH}$, the gate will attract electrons, including an n-type conductive channel in the substrate below the oxide. Electrons will flow between n-doped terminals and the switch will be on.

The tight-binding method has been used to calculate the biased energy of BLGs, which indicates energy dispersion of BLG as follows [29, 30]:

$$E(K) = \frac{V_1 + V_2}{2} \pm \sqrt{\varepsilon_k^2 + \frac{V^2}{4} + \frac{t_\perp^2}{2} \pm \frac{1}{2}\sqrt{4\left(V^2 + t_\perp^2\right)\epsilon_k^2 + t_\perp^4}}, \tag{2}$$

where ϵ_k is the electron's dispersion in monolayer graphene and $t_\perp = 0.32$ eV is the interlayer hopping energy. The wave vector in which the smallest gap is observed is given by

$$k_g = \frac{V}{2\nu_F\hbar}\sqrt{\frac{V^2 + 2t_\perp^2}{V^2 + t_\perp^2}}, \tag{3}$$

where the $\nu_F \approx 1 \times 10^6$ m·s^{-1} is the Fermi velocity [5] and $\hbar$ is the reduced Planck constant. Near k_g the energy dispersion can be written as [31]

$$E(k) = \frac{E_g}{2} + \frac{\hbar^2}{2m^*}\left(|k| - k_g\right)^2 + \frac{V_1 + V_2}{2}, \tag{4}$$

where $k = k_x\hat{i} + k_y\hat{j}$ and m^* is the effective mass in BLG. The density of states for BLG which indicates the number of states for each interval of energy at each energy level that can be occupied by electrons can be written as

$$\mathrm{DOS} = \frac{\Delta n}{A\Delta E} = \left(\frac{\hbar^2}{m^*}\frac{(k - k_g)}{k}2\pi\right)^{-1} = \frac{km^*}{2\pi\hbar^2\left(k - k_g\right)}. \tag{5}$$

The velocity of electrons is directly proportional to the value of DOS at any instance. Average velocity of carriers in the first subband in bilayer graphene can be obtained by the accumulative velocity of all carriers divided by the number of carriers. The carrier drift velocity has been reported to be formulated in the following form [32]:

$$\nu = \int \frac{|\nu|\,\mathrm{DOS}(E)\,F(E)\,dE}{n}. \tag{6}$$

From the kinetic energy principle, $|\nu| = \sqrt{2E/m}$, DOS(E) is density of states, $F(E) = 1/(1 + e^{(E-E_f)/K_BT})$ is the Fermi-Dirac distribution function which gives the probability of

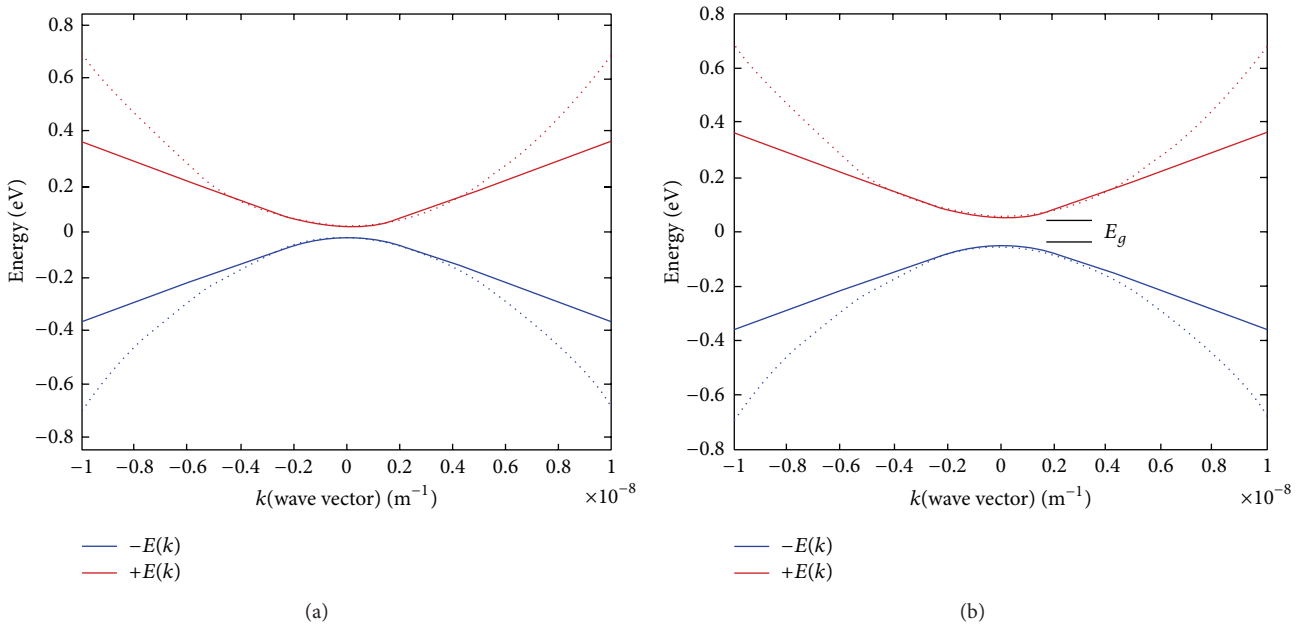

FIGURE 2: Band structure of BLG near the Dirac points for (a) $V = 0$ (unbiased BLG) and (b) $V \neq 0$ (biased BLG) [25].

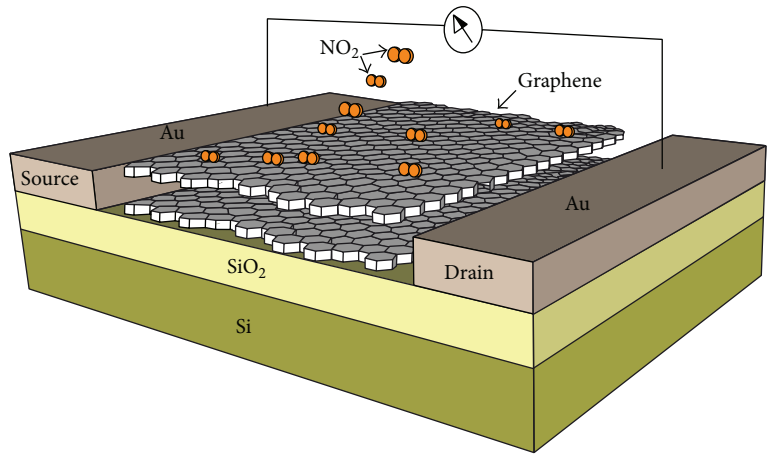

FIGURE 3: Proposed structure of gas sensor based on bilayer graphene.

occupation of a state at any energy level, and n is carrier concentration [33]. Hence, the integral of the numerator in (6) with respect to E can be rewritten as

$$\int |\nu| \,\mathrm{DOS}\,(E)\, F\,(E)\, dE = \frac{1}{\pi\hbar^2} \int \frac{Ek}{\left(k - k_g\right)} \frac{1}{1 + e^{(E-E_f)/k_BT}} dE, \tag{7}$$

where $k = \pm\left[2m^*(E - E_c)/\hbar^2\right]^{1/2} + k_g$, giving

$$\int |\nu| \,\mathrm{DOS}\,(E)\, F\,(E)\, dE = \frac{1}{\pi\hbar^2} \left(\int \frac{E}{1 + e^{(E-E_f)/K_BT}} dE + \frac{k_g\hbar}{\sqrt{2m^*}} \int \frac{(E - E_c)^{-1/2}}{1 + e^{(E-E_f)/K_BT}} dE \right). \tag{8}$$

It has been attempted to write (8) in a form which can be solved using the Fermi integrals. The obtained equation is as follows:

$$\int |\nu| \,\mathrm{DOS}\,(E)\, F\,(E)\, dE = \frac{(K_BT)^2}{\pi\hbar^2} \int \frac{x}{1 + e^{(x-\eta)}} dx + \frac{K_BTE_c}{\pi\hbar^2} \int \frac{dx}{1 + e^{(x-\eta)}} + \frac{K_BTk_g\hbar}{\pi\hbar^2\sqrt{2m}\sqrt{K_BT}} \int \frac{x^{-1/2}}{1 + e^{(x-\eta)}} dx \tag{9}$$

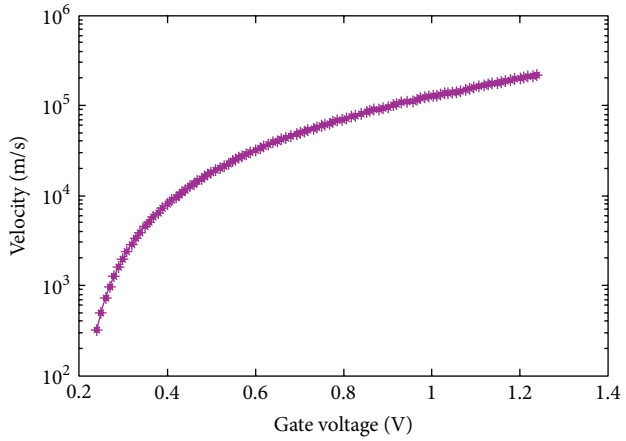

Figure 4: The velocity of BLG.

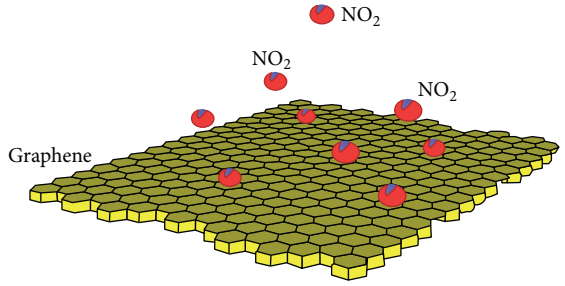

Figure 5: Schematic of NO_2 adsorption processes by surface area of graphene.

in which the orders of x in the numerator of the integrands are 1, 0, and $-1/2$, thus making the integrals equivalent to the Fermi integrals of orders 1, 0, and $-1/2$, respectively. This can finally give the following equation [34]:

$$\nu = \left[\frac{(K_B T)^2}{\pi\hbar^2} f(1) + \frac{K_B T E_c}{\pi\hbar^2} f(0) + \frac{K_B T k_g}{\pi\hbar\sqrt{2mK_B T}} f\left(-\frac{1}{2}\right) \right] \times n^{-1}, \tag{10}$$

in which $f(1)$, $f(0)$, and $f(-1/2)$ are the Fermi integral of orders 1, 0, and $-1/2$, respectively. For the details on the derivation and mathematical representation of the Fermi integrals, the reader is referred to [34]. Velocity is evaluated in Figure 4 based on (10) [35].

As can be seen in Figure 5, when the sensor is exposed to gas, according to the chemical reaction between graphene and gas molecules, graphene experiences a change in the velocity of its carriers which can in turn cause alterations in the current and channel voltage. In other terms, the electron exchange between the gas and the surface of the graphene creates new carriers which change the velocity of electrons [36].

It can be concluded that the velocity of electrons in the presence of gas is equal to that of the no-gas state plus the

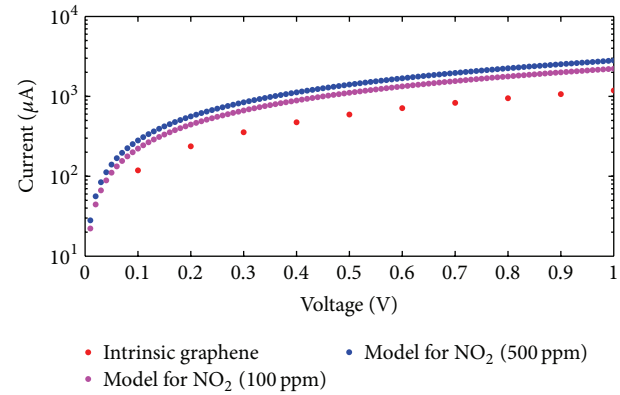

Figure 6: The comparison of current-voltage characteristics for 100 ppm and 500 ppm and intrinsic graphene based on proposed model.

velocity change when graphene is exposed to gas. Consider the following:

$$\nu_{\text{with gas}} = \nu_{\text{without gas}} + \nu_{\text{gas injected}}. \tag{11}$$

From this, the current-voltage relation can be derived as follows:

$$I = nq\nu A, \tag{12}$$

where n is charge carrier density, q is electrical charge, ν is drift velocity of the charge carriers, and A is the area in which the charges are moving. In Figure 6, the current-voltage characteristic of intrinsic graphene exposed to ambient air only as well as the current-voltage characteristic of BLG based NO_2 sensor for graphene under 100 ppm and 500 ppm NO_2 concentration is plotted. By current-voltage characteristic of the presented model, it is demonstrated that current of gas sensor rises with increasing the NO_2 concentration. Therefore, it is notable that, based on the supposed model sensor, I-V characteristic is controlled by NO_2 concentration.

When the sensor is exposed to the gas, the density of states can be divided into two parts; one is the density of states without gas $\text{DOS}_{\text{WOG}}(E)$ and the second parameter is the density of states with gas proportional to αF, which depends on different values of NO_2 gas concentration. Consider the following:

$$\text{DOS} = \text{DOS}_{\text{WOG}} + \text{DOS}_{\text{gas injected}}, \tag{13}$$

where $\text{DOS}_{\text{gas injected}} \approx \alpha F$.

In our study, α is our control parameter; that is, by heuristically changing the values of α, we attempt to set the results from the proposed model as close to the experimental results as possible. According to the relation between the

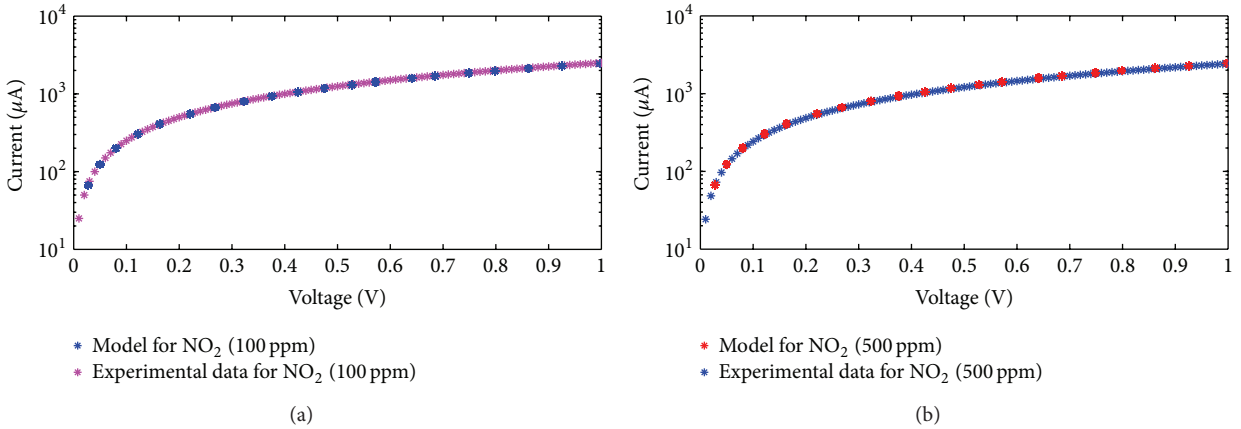

Figure 7: The current-voltage characteristics for (a) 100 ppm and (b) 500 ppm.

Table 1: Different F values with α parameter.

Carrier concentration (F)	Parameter (α)
100 ppm	0.077
500 ppm	0.016

control parameter and density of states, we can write the following:

$$\begin{aligned}\nu_{\text{total}} &= \left[\frac{(K_BT)^2}{\pi\hbar^2}f(1) + \frac{K_BTE_c}{\pi\hbar^2}f(0)\right. \\ &\quad + \frac{K_BTk_g}{\pi\hbar\sqrt{2mK_BT}}f\left(-\frac{1}{2}\right) + \frac{2\alpha F}{m^*}(K_BT)^2 f(1) \\ &\quad \left. + \frac{2\alpha F}{m^*}K_BTE_c f(0)\right] \times n^{-1},\end{aligned} \tag{14}$$

where n is the carrier concentration equal to $n = 10^{16}$ for two-dimensional bilayer graphene [35].

The velocity of the graphene-based FET devices is influenced by the number of carriers changing in the channel. FET-based graphene with high sensitivity was applied to detect the NO_2 gas, based on velocity variations. As depicted in Figures 7(a) and 7(b), the velocity of channel will change due to the adsorption of NO_2 to the surface of the FET channel. The performance of graphene-based gas sensor under exposure of 100 ppm and 500 ppm of NO_2 gas is evaluated and the analytical results of the proposed model for gas sensor with appropriate parameters are compared with the experimental data extracted from [16] which shows a good agreement. It is evident in the figure that the points calculated and obtained from our model satisfactorily coincide with the measurement data.

In the suggested model, different carrier concentrations are demonstrated in the form of α parameter which is presented in Table 1.

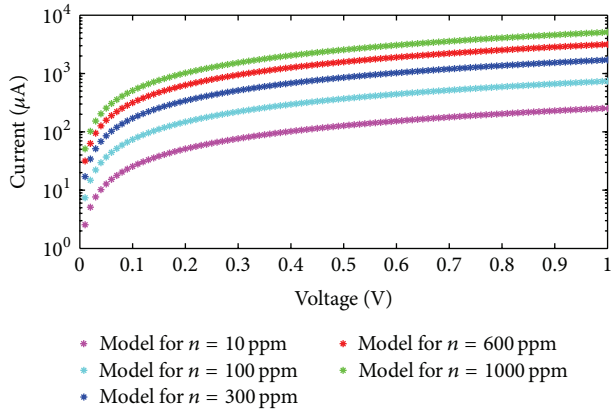

Figure 8: I-V characteristic of different values of NO_2 carrier concentration.

According to the analytical model, α is proposed as the controlling parameter of gas concentration. The analytic model based on data extracted can be written as follows:

$$\alpha = ae^{bx}. \tag{15}$$

Referring to the analytical model, the velocity will be enhanced as the amount of gas concentration increases. According to the extracted data, parameters a and b are calculated as $a = 0.370$ and $b = -1.57$.

It is evident in Figure 8 that I-V characteristic curve can be controlled by the carrier concentration factor. The current rises as a result of increase in the carrier concentration.

3. Conclusion

Graphene indicates amazing carrier transport properties and high sensitivity at the single molecule level which makes it a promising material for nanosensor applications. An innovative analysis of matching models using different values has been presented in this work to verify that the conductance of the graphene-based gas sensor is increased at higher carrier concentrations. NO_2 gas effect in the FET channel

region in the form of carrier density variation influencing the carrier velocity is further modelled, and current-voltage characteristic of a bilayer graphene (BLG) as a NO_2 gas sensor is reported. Injected carriers from NO_2 on the carrier concentration of bilayer graphene surface are monitored. Furthermore, injected carriers as a function of gas concentration (f) are demonstrated. It was shown that, as carrier concentration increases, the control parameter, α, decreases. Finally, for the purpose of verification, I-V characteristic of gas sensor in exposure to NO_2 is investigated and a comparative study between the model and experimental data from literature shows an acceptable agreement.

Conflict of Interests

The authors declare that there is no conflict of interests regarding the publication of this paper.

Acknowledgments

The authors would like to thank Ministry of Education Malaysia and Universiti Teknologi Malaysia for funding this research project through a research Grant (GUP-04H40) titled "Dimension Reduction & Data Clustering for High Dimensional & Large Datasets".

References

[1] M. Ettore, V. la Ferrara, M. Mara, T. Polichetti, N. Ivana, and G. di Francia, "Gas sensors based on graphene: comparison of two different fabrication approaches," *Chimica Oggi*, vol. 29, no. 1, pp. 39–41, 2011.

[2] H. Yu, P. Xu, X. Xia et al., "Micro-/nanocombined gas sensors with functionalized mesoporous thin film self-assembled in batches onto resonant cantilevers," *IEEE Transactions on Industrial Electronics*, vol. 59, no. 12, pp. 4881–4887, 2012.

[3] E. Akbari, M. T. Ahmadi, M. J. Kiani et al., "Monolayer graphene based CO_2 gas sensor analytical model," *Journal of Computational and Theoretical Nanoscience*, vol. 10, no. 6, pp. 1301–1304, 2013.

[4] B. Huang, Z. Li, Z. Liu et al., "Adsorption of gas molecules on graphene nanoribbons and its implication for nanoscale molecule sensor," *Journal of Physical Chemistry C*, vol. 112, no. 35, pp. 13442–13446, 2008.

[5] M. Zhou, Y.-H. Lu, Y.-Q. Cai, C. Zhang, and Y.-P. Feng, "Adsorption of gas molecules on transition metal embedded graphene: a search for high-performance graphene-based catalysts and gas sensors," *Nanotechnology*, vol. 22, no. 38, Article ID 385502, 2011.

[6] E. Akbari, M. T. Ahmadi, Y. Rubiyah, M. H. Ghadiry, and M. Saeidmanesh, "Gas concentration effect on channel capacitance in graphene based sensors," *Journal of Computational and Theoretical Nanoscience*, vol. 10, no. 10, pp. 2449–2452, 2013.

[7] H. Jiang, "Chemical preparation of graphene-based nanomaterials and their applications in chemical and biological sensors," *Small*, vol. 7, no. 17, pp. 2413–2427, 2011.

[8] S. Kochmann, T. Hirsch, and O. S. Wolfbeis, "Graphenes in chemical sensors and biosensors," *TrAC Trends in Analytical Chemistry*, vol. 39, 2012.

[9] E. Akbari, R. Yousof, M. T. Ahmadi et al., "The effect of concentration on gas sensor model based on graphene nanoribbon," *Neural Computing and Applications*, vol. 24, no. 1, pp. 143–146, 2014.

[10] S. Okude, "Detection of chemical reactivity of intramolecular atom involves setting arbitrary atoms of intramolecular atom to alpha, and calculating magnitude of value of difference of preset parameter as index of chemical reactivity".

[11] M. Rahmani, "Analytical modeling of monolayer graphene-based NO_2 sensor," *Sensor Letters*, vol. 11, no. 2, pp. 270–275, 2013.

[12] O. Leenaerts, B. Partoens, and F. M. Peeters, "Adsorption of H_2O, NH_3, CO, NO_2, and NO on graphene: a first-principles study," *Physical Review B—Condensed Matter and Materials Physics*, vol. 77, no. 12, Article ID 125416, 2008.

[13] Y.-H. Zhang, Y.-B. Chen, K.-G. Zhou et al., "Improving gas sensing properties of graphene by introducing dopants and defects: a first-principles study," *Nanotechnology*, vol. 20, no. 18, Article ID 185504, 2009.

[14] X.-L. Wei, Y.-P. Chen, W.-L. Liu, and J.-X. Zhong, "Enhanced gas sensor based on nitrogen-vacancy graphene nanoribbons," *Physics Letters A: General, Atomic and Solid State Physics*, vol. 376, no. 4, pp. 559–562, 2012.

[15] S. Hadlington, "Graphene sensor achieves ultimate sensitivity," *Chemistry World*, vol. 4, no. 9, p. 29, 2007.

[16] G. Ko, H.-Y. Kim, J. Ahn, Y.-M. Park, K.-Y. Lee, and J. Kim, "Graphene-based nitrogen dioxide gas sensors," *Current Applied Physics*, vol. 10, no. 4, pp. 1002–1004, 2010.

[17] A. Das, B. Chakraborty, and A. K. Sood, "Probing single and bilayer graphene field effect transistors by Raman spectroscopy," *Modern Physics Letters B*, vol. 25, no. 8, pp. 511–535, 2011.

[18] K.-T. Lam, C. Lee, and G. Liang, "Bilayer graphene nanoribbon nanoelectromechanical system device: a computational study," *Applied Physics Letters*, vol. 95, no. 14, Article ID 143107, 2009.

[19] S. M. Mousavi, M. T. Ahmadi, J. F. Webb et al., "Bilayer graphene nanoribbon carrier statistics in the degenerate regime," in *Proceedings of the 4th Global Conference on Power Control and Optimization*, pp. 180–183, December 2010.

[20] M. T. A. M. J. Kiani, E. akbari, M. Rahmani, H. karimi, and F. K. C. harun, "Analytical modeling of bilayer graphene based biosensor," *Journal of Computational and Theoretical Nanoscience (CTN)*, 2012.

[21] H. Hatami, N. Abedpour, A. Qaiumzadeh, and R. Asgari, "Conductance of bilayer graphene in the presence of a magnetic field: effect of disorder," *Physical Review B—Condensed Matter and Materials Physics*, vol. 83, no. 12, Article ID 125433, 2011.

[22] T. Yu, E.-K. Lee, B. Briggs, B. Nagabhirava, and B. Yu, "Reliability study of bilayer graphene—material for future transistor and interconnect," in *Proceedings of the IEEE International Reliability Physics Symposium (IRPS '10)*, pp. 80–83, May 2010.

[23] N. A. Amin, M. T. Ahmadi, Z. Johari, S. M. Mousavi, and R. Ismail, "Effective mobility model of graphene nanoribbon in parabolic band energy," *Modern Physics Letters B*, vol. 25, no. 10, pp. 739–745, 2011.

[24] M. T. Ahmadi, Z. Johari, N. A. Amin, A. H. Fallahpour, and R. Ismail, "Graphene nanoribbon conductance model in parabolic band structure," *Journal of Nanomaterials*, vol. 2010, Article ID 753738, 4 pages, 2010.

[25] M. T. Ahmadi, Z. Johari, N. A. Amin, and R. Ismail, "Band energy effect on carrier velocity limit in graphene nanoribbon," *Journal of Experimental Nanoscience*, vol. 7, no. 1, pp. 62–73, 2012.

[26] J. Nilsson, A. H. C. Neto, F. Guinea, and N. M. R. Peres, "Electronic properties of bilayer and multilayer graphene," *Physical Review B—Condensed Matter and Materials Physics*, vol. 78, no. 4, Article ID 045405, 2008.

[27] E. F. W. Olthuis, K. Erik, and A. van den Berg, *Sensing with FETs—Once, Now and Future*, UTpublications, 2007.

[28] F. Schwierz, "Graphene transistors," *Nature Nanotechnology*, vol. 5, no. 7, pp. 487–496, 2010.

[29] M. Cheli, G. Fiori, and G. Iannaccone, "A semianalytical model of bilayer-graphene field-effect transistor," *IEEE Transactions on Electron Devices*, vol. 56, no. 12, pp. 2979–2986, 2009.

[30] M. Rahmani, R. Ismail, M. T. Ahmadi et al., "The effect of bilayer graphene nanoribbon geometry on schottky-barrier diode performance," *Journal of Nanomaterials*, vol. 2013, Article ID 636239, 8 pages, 2013.

[31] J. I. Väyrynen and T. Ojanen, "Electronic properties of graphene multilayers," *Physical Review Letters*, vol. 107, no. 10, Article ID 109901, 2011.

[32] M. T. Ahmadi, R. Ismail, M. L. P. Tan, and V. K. Arora, "The ultimate ballistic drift velocity in carbon nanotubes," *Journal of Nanomaterials*, vol. 2008, no. 1, Article ID 769250, 2008.

[33] M. T. Ahmadi and R. Ismail, "Graphene nanoribbon fermi energy model in parabolic band structure," in *Proceedings of the UKSim/AMSS 1st International Conference on Intelligent Systems, Modelling and Simulation (ISMS '10)*, pp. 401–405, January 2010.

[34] R. Kim and M. Lundstrom, *Notes on Fermi-Dirac Integrals*, 2nd edition, 2008.

[35] M. Saeidmanesh, M. T. Ahmadi, and M. H. Ghadiry, "Perpendicular electric field effect on bilayer graphene carrier statistic," *Journal of Computational and Theoretical Nanoscience*, vol. 10, no. 9, 2013.

[36] J. Xia, F. Chen, J. Li, and N. Tao, "Measurement of the quantum capacitance of graphene," *Nature Nanotechnology*, vol. 4, no. 8, 509 pages, 2009.